

# CHARACTERIZATION OF CANDIDATE VEHICLE STATES FOR XNAV SYSTEMS

Kevin G. Lohan\* and Zachary R. Putnam†

This paper presents the framework for finding intersections of an infinite set of wavefronts from pulsars in 2D. The conditions for an intersection to exist are shown along with a numeric scheme for rapidly determining intersection feasibility. The numeric scheme reduces the dimensionality of the problem by one resulting in a much more computationally efficient solution. Using this algorithm the candidate intersections for 3, 4, or 5 pulsars is found for a phase tolerance between  $10^{-3}$  and  $10^{-5}$ . It was found that to minimize the number of candidate positions within a given domain it is more beneficial to increase the number of pulsars observed rather than decrease the measurement uncertainty. An additional solution is found analytically by solving the mixed-integer math problem. However this solution does not incorporate any measurement error and there is no way to know how many function evaluations are required to find all solutions within a domain.

## INTRODUCTION

X-ray pulsar based navigation (XNAV) is means of autonomous navigation in space. XNAV has shown promise as an autonomous system,<sup>1-4</sup> an integrated system,<sup>5,6</sup> or for the relative position between constellations of satellites.<sup>7</sup> XNAV has two main benefits relative to the current state of the art Deep Space Network (DSN): (1) XNAV is nearly autonomous, i.e. navigation tasks may be performed onboard a spacecraft without the need for communication with an Earth-based ground station. (2) XNAV is more accurate than the DSN at distances from Earth beyond approximately 15 AU.

The Majority of XNAV applications operate under a relative position update framework. A brief outline of the state update is given as follows.<sup>8,9</sup> To generate an XNAV measurement, a pulsar is observed for a given length of time and all x-ray photons which reach the detector are recorded. Using an initial position estimate, the photon arrival times are then moved from the vehicle's frame of reference to a reference epoch. At the reference epoch the phase evolution of the pulsars are well known and may be propagated into the future. The photon time of arrivals may be compared to the phase at the epoch to determine a phase offset relative to the reference. This phase offset is then used to generate a position update in the direction of the pulsar.

A key limitation of this method is that it requires an initial position estimate. Without that estimate, the photon time of arrivals can not be shifted back to the reference epoch. Sheikh et al

---

\*Graduate Research Assistant, Aerospace Engineering, University of Illinois at Urbana-Champaign, MC-236, 104 S. Wright Street.

†Assistant Professor, Aerospace Engineering, University of Illinois at Urbana-Champaign, MC-236, 104 S. Wright Street

developed an alternate solution strategy which they called absolute position determination.<sup>10</sup> This method uses measurement difference to construct a set of candidate wavefronts for each pulsar measurement. The vehicle location must be at a point where all wavefronts intersect. Currently these types of systems are not considered for navigation due to the increased complexity required for measuring multiple pulsars simultaneously.

This research further expands upon the absolute position update method to characterize how the candidate intersections evolve with error and number of pulsar observations. The problem formulation for the intersection of infinite sets of lines is presented along with criteria to determine candidate set intersections. An analytic solution to the mixed-integer math problem is shown for a simplified test case. A numeric algorithm to rapidly iterate through candidate solutions is presented.

## IDENTIFICATION OF CANDIDATE POSITIONS IN TWO DIMENSIONS

During the XNAV state update process, the vehicle generates a phase offset with respect to an expected phase. A position update can be generated based on the phase offset, a first order approximation of which is given by,

$$\frac{\mathbf{n} \cdot \Delta \mathbf{r}}{c} = \Delta t \quad (1)$$

Here the position update,  $\mathbf{n} \cdot \Delta \mathbf{r}$ , is in the direction of the pulsar. Since the distance between pulsars and our solar system is large, pulsars may be assumed to be infinitely far from the solar system, making the pulsar waveform appear to propagate as a plane. The position update may then be determined in the direction of the pulsar. In the absolute position framework, no initial position estimate is available, so there is no way to distinguish between peaks of the pulsar waveform. The phase measurement only restricts vehicle position to an infinite set of planes perpendicular to the direction of the pulsar. If an initial position estimate exists, it may be used to identify which plane the vehicle should be located. A second pulsar may be observed to determine the vehicle position with respect to another direction which places the vehicle on a second set of infinite planes. Combining these two measurements puts the vehicle somewhere on the intersection of the two series of planes, resulting in an infinite set of lines. A third pulsar measurement reduces this space to an infinite set of points, and any subsequent measurement decreases the number of candidates intersections within a given volume of space.

We now reduce the problem to two dimensions (2D) for the following reasons:

1. Most in-space trajectories are planar.
2. The three-dimensional problem quickly reduces to finding intersections of lines, a feature preserved in two dimensions.
3. Computational time is significantly reduced in two dimensions.

Figure 1 illustrates the candidate position identification problem in two dimensions: the lines are the projections of the planar wavefronts. Figure 1a shows intersections between two pulsar wavefronts; Figure 1b shows intersections resulting from three pulsar wavefronts. Further, error in the pulsar position estimate will be assumed to be independent of position. In this study we consider the following pulsars to determine position: J0218+4232, J0030+0451, B1937+21, B18218-24, and

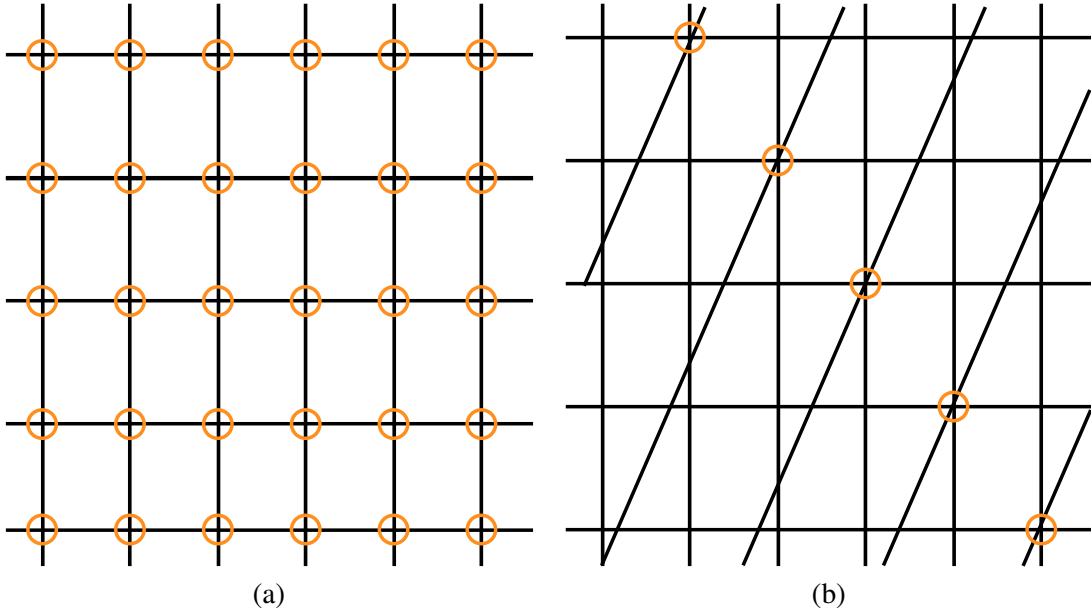


**Figure 1. (a) Intersections of two sets of lines (b) Intersections of three sets of lines**

Pulsar	J0218+4232	J0030+0451	B1937+21	B18218-24	J0437-4715
Period [s]	0.0023	0.0049	0.0016	0.0031	0.0058
Normal Vector	$\begin{bmatrix} 0.701 \\ 0.713 \end{bmatrix}$	$\begin{bmatrix} 0.535 \\ 0.845 \end{bmatrix}$	$\begin{bmatrix} 0.168 \\ -0.986 \end{bmatrix}$	$\begin{bmatrix} -0.0451 \\ 0.999 \end{bmatrix}$	$\begin{bmatrix} -0.267 \\ 0.964 \end{bmatrix}$
Wavefronts	40,990	18,774	48,086	22,452	14,146

**Table 1. Candidate pulsar properties**

J0437-4715. These are the candidate set of pulsars for NASA's SEXTANT experiments.<sup>1</sup> The search domain for the spacecraft position is restricted to a square with sides of length  $2 \times 10^{10}$ m. This domain size is approximately 2/15ths of an AU and the resulting number of wavefronts for each pulsar are given in Table 1. Candidate intersections may be found as follows:

The standard form of a 2D line is given by

$$ax + by = c \quad (2)$$

Where  $c$  characterizes the line, and is defined by a point on the line

$$c = ax_0 + by_0 \quad (3)$$

A set of lines for each pulsar measurement may be defined and used to generate a system of equations all of the form

$$b_i x + a_i y = c_i \quad (4)$$

Where  $i$  is the index of the pulsar. The intersection of two pulsars results in the linear system given below

$$\begin{bmatrix} b_1 & a_1 \\ b_2 & a_2 \end{bmatrix} \begin{bmatrix} x \\ y \end{bmatrix} = \begin{bmatrix} c_1 \\ c_2 \end{bmatrix} \quad (5)$$

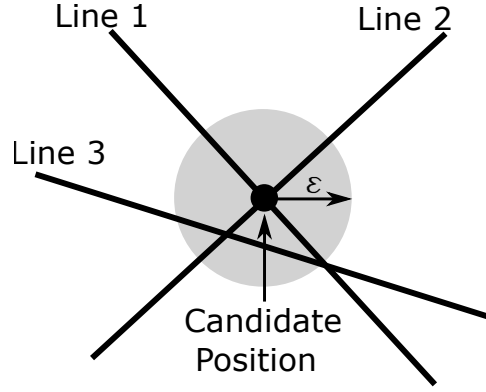


**Figure 2. Feasible region for the intersection of an additional pulsar**

where  $a$  and  $b$  are the normal vector components

$$\mathbf{n}_i = \begin{bmatrix} a_i \\ b_i \end{bmatrix} \quad i = 1 : 2 \quad (6)$$

Equation 3 is the dot product of the normal vector with a point on the plane. For this application, the point on the plane is the normal vector multiplied by the distance between wavefronts, or the wavelength. For a given wavefront, the constant is given by

$$c_i = cT_i i = \lambda_i i \quad (7)$$

A phase offset may be added to the index

$$c_i = \lambda_i(i + \phi_i) \quad (8)$$

For each additional observed pulsar the  $(x, y)$  candidate point must satisfy Equation 4 for the new pulsar.

## NUMERIC CANDIDATE DETERMINATION

### Numerically Evaluating Candidate Positions

To check if the wavefronts from an additional pulsar coincide with a given intersection, Equation 4 must be valid when evaluated at a candidate intersection point. From Equation 4, the coefficient  $c$  may be moved to the left hand side and the right hand side may be interpreted as the distance from the new wavefront to the intersection point, as shown in Equation 9. If the right hand side is less than some tolerance,  $\epsilon$ , the intersection point is a candidate vehicle position, see Figure 2. The tolerance may be set to represent the phase accuracy of the pulsar waveform measurement.

$$a_j x + b_j y - c_j \leq \epsilon \quad j = 3, 4, \dots \quad (9)$$

If this condition is checked for each candidate point then  $\prod_{i=1}^j N_i$  computations are required where the  $N_i$  correspond to the number of pulsar wavefronts in the search space, and  $j$  is the number

of pulsars observed. Solving the problem in this manner is inefficient and may be intractable given the limitations of flight computers, especially if the search domain is large. A more efficient method of determining the feasibility of a candidate intersection is to determine the required  $c_j$  value for an intersection to exist by solving Equation 4 for a given candidate position. Looking back to Equation 8, it can be seen that this value is related to the period of the pulsar, its phase offset, and an integer index. Equation 8 may be solved for the integer index as

$$i = \frac{c_j}{\lambda_i} - \phi_i \quad (10)$$

The required  $c_j$  and other pulsar properties are substituted into this equation, and if the value of  $i$  is integral, then the pulsar wavefront will intersect at this candidate location. Otherwise, there will be no intersection. By performing the computation this way, there are now only  $\prod_{i=1}^{j-1} N_i$  computations which corresponds to the number of candidate locations. If additional pulsars are observed, only the points which pass the previous test are considered, further reducing the computational load.

### Resulting Candidate Intersections

The number of candidate points in the search domain is dependent on the error in phase which in turn depends on observation time. The error in phase may be defined by the Cramer-Rao lower bound which places a bound on the variance of an unbiased estimator. Golshan et al derived this quantity for pulsar based navigation in terms of the observation time, pulsar waveform, the derivative of the waveform, and the source and background photon arrival rates.<sup>11</sup> For a given pulsar this expression relates the observation time with the phase error. This may be used to define the acceptable tolerance  $\epsilon$  for candidate intersections.

$$\begin{aligned} \text{Var}(\hat{\theta}_0) &\geq \left[ T_{obs} \int_0^1 \frac{[\alpha h'(\phi)]^2}{\alpha h(\phi) + \beta} d\phi \right]^{-1} \\ \text{Var}(\hat{\tau}) &\geq \left[ f^2 T_{obs} \int_0^1 \frac{[\alpha h'(\phi)]^2}{\alpha h(\phi) + \beta} d\phi \right]^{-1} \end{aligned} \quad (11)$$

A few additional assumptions were made to simplify the problem. All measurements are assumed to be measured concurrently to allow for the calculation of their intersections. Based on how the problem has been defined, the intersection of two wavefronts are found first then an error ball is constructed from this point, Figure 2. The size of the error ball is related to the uncertainty in the measurement of an additional pulsar. The error of the first two measurements would correspond to shifting the center of the error ball not increasing the size of the ball. Therefore, the error in the first two pulsar observations is not included. To enforce a solution within the domain no phase offset is given for any of the pulsars resulting in a solution at the origin.

Using a phase tolerance of  $10^{-5}$  the intersections of the first three and four pulsars may be found as shown in Figure 3. The phase error of  $10^{-5}$  results in a position error on the order of 10 m. This small position error results in 1,663 candidate solutions within the space. The distribution of these points spans the entire search domain nearly uniformly. Since each of these points is a feasible solution to within 10 m there is no way of accurately determining at which point the observer is located. There are two options to then resolve position: the pulsars may be observed for a larger period of time to reduce the position error and accept fewer candidate positions, or another pulsar

may be observed. If an additional pulsar is observed the 1,663 solutions may be reduced to a single solution at the origin. However, it should be noted that, in general, there is no guarantee that a solution exists in a domain of this size. The addition of a small phase offset to the problem may result in no solution within the domain.

The same procedure may be repeated with other phase tolerances to determine how the candidate solutions change with phase accuracy. If the phase tolerance is adjusted to  $10^{-4}$ , which would be a position error on the order of 100 m, there would be 16,559 solutions for three pulsars and 3 solutions for four pulsars, Figure 4. The three pulsar solutions are not shown since they would cover the entire background. Comparing the  $10^{-4}$  case to the  $10^{-5}$  case it can be seen that decreasing the phase tolerance by an order of magnitude increased the number of candidate solutions by an order of magnitude for the intersection of 3 pulsars. For the fourth pulsar the number of solutions only increased from 1 to 3. Adding a fifth pulsar may fully resolve the position, or perhaps the spacing is large enough to resolve the position of the spacecraft using other available information, e.g. the spacecraft is known to be in orbit about a particular body.

A final case may be considered where the pulsar is observed for a phase tolerance of  $10^{-3}$  resulting in a position error on the order of 1 km. In this case there are 165,667 solutions for three pulsars and 329 solutions for four pulsars, Figure 5(a). Again the reduction of phase tolerance by an order of magnitude increased the number of candidate solutions by an order of magnitude for three pulsars but it increased the number of solutions by two orders of magnitude for four pulsars. It can also be seen that the solutions to the four pulsar case are not uniformly distributed as the 3 pulsar solutions were for the  $10^{-5}$  phase tolerance. Here the solutions are constrained to bands whose thickness is not constant and whose direction is not in the direction of any of the pulsars. It was mentioned that for the  $10^{-5}$  case adding a small phase offset moves the point outside of the domain. For this case if a small phase offset is added the same type of banded structure is retained however the bands are shifted. Figure 5(b) shows this for the case where time is shifted forward by 10 s.

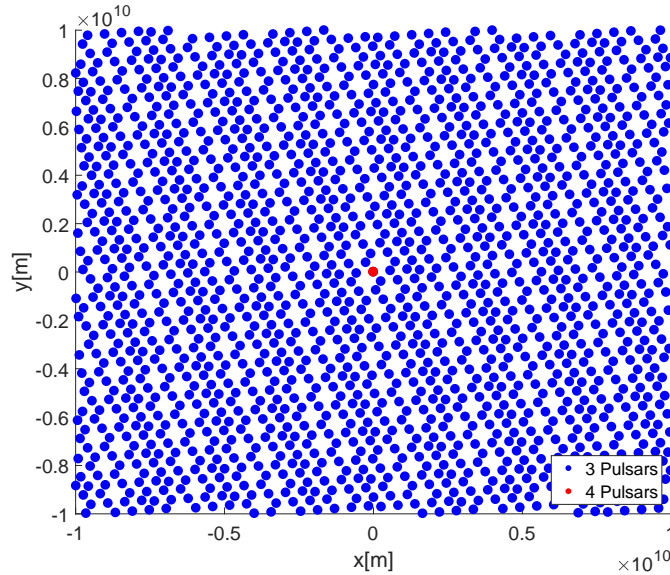


**Figure 3. Candidate vehicle positions for 3 and 4 pulsars within a phase tolerance of  $10^{-5}$**

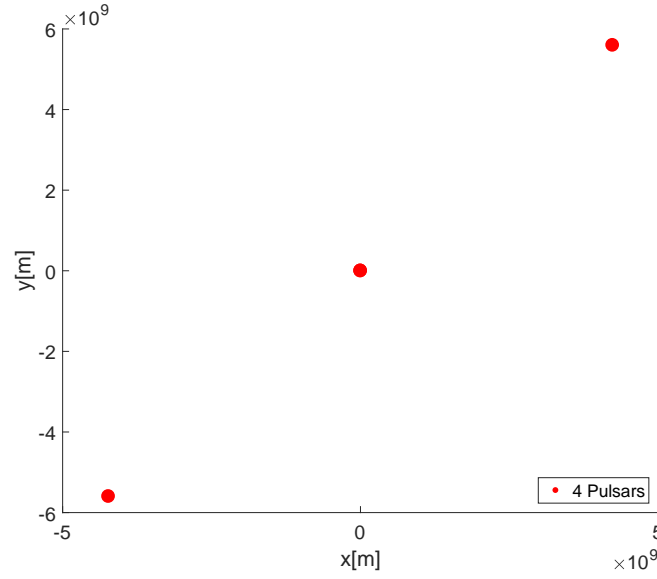


**Figure 4.** Candidate vehicle positions for 4 pulsars within a phase tolerance of  $10^{-4}$

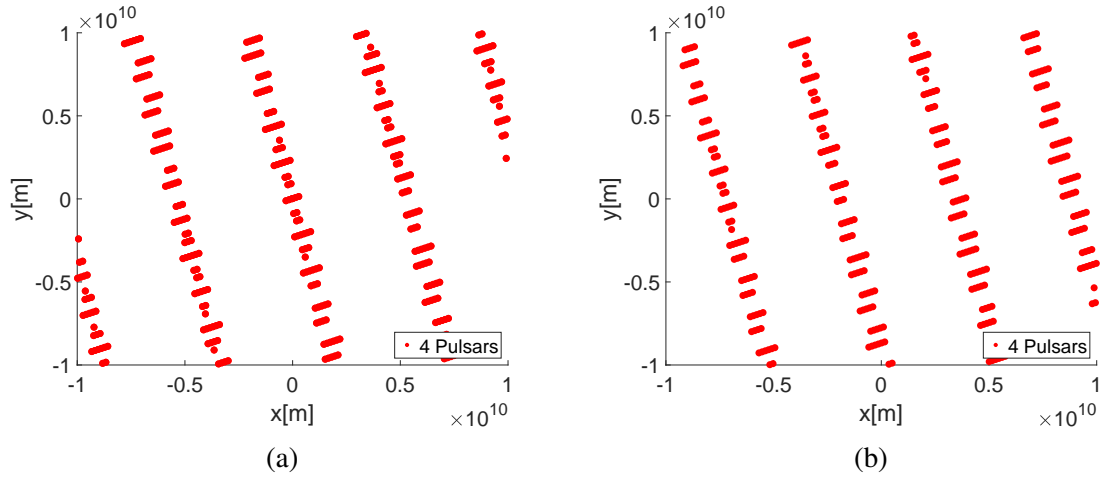


**Figure 5.** Candidate vehicle positions for 4 pulsars within a phase tolerance of  $10^{-3}$  with (a)  $t=0$  (b)  $t=10$  s

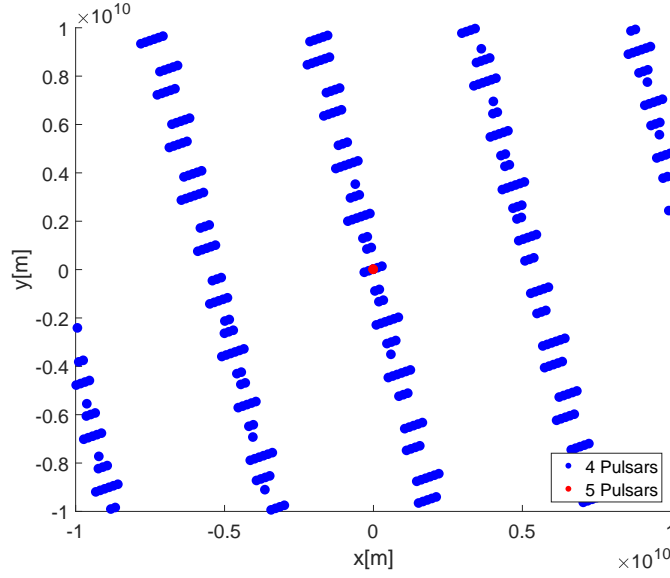


**Figure 6. Candidate vehicle positions for 4 and 5 pulsars within a phase tolerance of  $10^{-3}$**

Phase Tolerance	J0218+4232	J0030+0451	B1937+21	B18218-24	J0437-4715
$10^{-3}$	$1.79 \times 10^5 \text{s}$	$1.85 \times 10^5 \text{s}$	$4.29 \times 10^4 \text{s}$	$4.19 \times 10^3 \text{s}$	$3.45 \times 10^5 \text{s}$
$10^{-4}$	$1.98 \times 10^7 \text{s}$	$1.85 \times 10^7 \text{s}$	$4.29 \times 10^6 \text{s}$	$4.19 \times 10^5 \text{s}$	$3.45 \times 10^7 \text{s}$
$10^{-5}$	$1.79 \times 10^9 \text{s}$	$1.85 \times 10^9 \text{s}$	$4.29 \times 10^8 \text{s}$	$4.19 \times 10^7 \text{s}$	$3.45 \times 10^9 \text{s}$

**Table 2. Required observation time to achieve the desired phase tolerance for each pulsar**

To further test this case a 5th pulsar may be added to the system which reduces the number of solutions to a single point at the origin, Figure 6. There are now two possible methods to obtain the solution at the origin. Either a phase tolerance of  $10^{-5}$  may be used for four pulsars, or a phase tolerance of  $10^{-3}$  may be used with five pulsars. Clearly a phase tolerance of  $10^{-4}$  and five pulsars would also yield the solution. When considering these two cases the time required to perform the computation is nearly identical since the original mesh is the same size. The initial mesh for both cases is  $40,990 \times 18,774$  which results in 769,546,260 initial candidates. These initial candidates are reduced to 1,663 for  $10^{-5}$  case, and 165,667 for the  $10^{-3}$  case which is negligible compared to the initial mesh. The important distinction here is how long it takes for the spacecraft to generate the required measurements.

Looking back to Equation 11 the variance is related to the observation time by  $1/T_{obs}$  which makes the error proportional to  $1/\sqrt{T_{obs}}$ . Furthermore the integral in the expression results in a constant for each pulsar which may be found in Ref. [12]. Using these parameters the observation time required for a phase tolerance of  $10^{-3}$ ,  $10^{-4}$ ,  $10^{-5}$  may be found and are shown in Table 2. Figure 7 shows the number of candidate solutions as a function of observation time for 3, 4 or 5 pulsar measurements. In order to determine the candidate set with a phase tolerance of  $10^{-3}$  a total observation time between  $4.07 \times 10^5$  and  $7.56 \times 10^5$  is required depending on the number of pulsars observed. A phase tolerance of  $10^{-4}$  requires between  $4.07 \times 10^7$  and  $7.56 \times 10^7$ , and a tolerance of  $10^{-5}$  between  $4.07 \times 10^9$  and  $7.56 \times 10^9$ . Measuring five pulsars at a phase tolerance of  $10^{-3}$



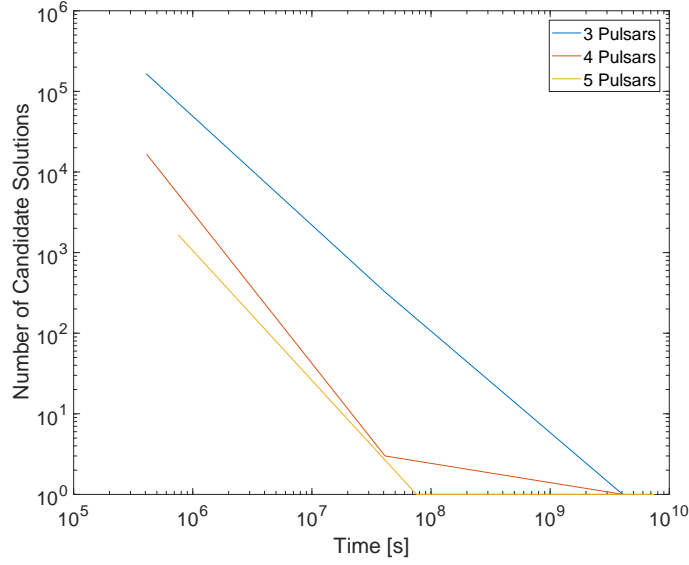


**Figure 7. Observation time vs number of candidate solutions for 3, 4 or 5 pulsar measurements.**

takes over 3 orders of magnitude less observation time than the required observation time for even one measurement at a phase tolerance of  $10^{-5}$ . Therefore, it may be more beneficial to observe additional pulsars rather than increase the observation time for each pulsar.

### ANALYTIC CANDIDATE DETERMINATION

An alternate approach to identify candidate positions is to frame the problem as a mixed-integer problem. The presented solution follows the form of Bowman and Burdet<sup>12</sup> whose solution represents the mixed-integer problem as an equivalent linear diophantine problem. The solution to these classes of problems may be found using reflexive generalized inverses as shown by Hurt and Waid.<sup>13</sup> Prior to solving the problem first it must be written in the correct form. For XNAV, the system of equations given by Equations 5 and 8 may be combined to form the set of equations

$$\begin{bmatrix} a_1 & b_1 \\ a_1 & b_2 \end{bmatrix} \begin{bmatrix} x \\ y \end{bmatrix} = \begin{bmatrix} \lambda_i(i + \phi_1) \\ \lambda_i(j + \phi_2) \end{bmatrix} \quad (12)$$

If a fourth pulsar is added to the system an additional row is added to the matrix equation

$$\begin{bmatrix} a_1 & b_1 \\ a_2 & b_2 \\ a_3 & b_3 \end{bmatrix} \begin{bmatrix} x \\ y \end{bmatrix} = \begin{bmatrix} \lambda_1(i + \phi_1) \\ \lambda_2(j + \phi_2) \\ \lambda_3(k + \phi_3) \end{bmatrix} \quad (13)$$

Each additional pulsar observed would add a row to the matrix equation. The standard form of a mixed integer problem is given by

$$A\mathbf{x} + B\mathbf{y} = \mathbf{c} \quad (14)$$

Where  $\mathbf{x}$  is a vector of integers,  $\mathbf{y}$  is a vector of scalars, and  $\mathbf{c}$  is a vector of rational numbers. Equation 13 may be rearranged into this form and is given by Equation 15 where  $\mathbf{x}$  is a vector of

integer indices,  $[i, j, k]^T$ , and  $\mathbf{y}$  is the vehicle position,  $[y_1, y_2]^T$ .

$$\begin{bmatrix} \lambda_1 & 0 & 0 \\ 0 & \lambda_2 & 0 \\ 0 & 0 & \lambda_3 \end{bmatrix} \mathbf{x} + \begin{bmatrix} a_1 & b_1 \\ a_2 & b_2 \\ a_3 & b_3 \end{bmatrix} \mathbf{y} = \begin{bmatrix} \lambda_1 \phi_1 \\ \lambda_2 \phi_2 \\ \lambda_3 \phi_3 \end{bmatrix} \quad (15)$$

Closed form solutions to equations of this form have been found for some cases.<sup>12</sup> The solutions are built around a reflexive generalized inverse of  $B$ , denoted as  $B^\#$ . A reflexive generalized inverse is not the same as a pseudo-inverse. The conditions for a pseudo-inverse are given by

$$BB^{-1}B = B \quad (16)$$

$$B^{-1}BB^{-1} = B^{-1} \quad (17)$$

$$(BB^{-1})^T = BB^{-1} \quad (18)$$

$$(B^{-1}B)^T = B^{-1}B \quad (19)$$

To be a reflexive generalized inverse, only the first two conditions are required. One important note is that for a reflexive generalized inverse,  $BB^\#$  or  $B^\#B$  is not necessarily equal to the identity matrix. If a reflexive generalized inverse of  $B$  can be found, then a pair of intermediate quantities may be defined

$$D = (I - BB^\#)A \quad (20)$$

$$\mathbf{d} = (I - BB^\#)\mathbf{c} \quad (21)$$

If the set of conditions:

$$D^\# \text{ is integral} \quad (22)$$

$$D^\# \mathbf{d} \text{ is integral} \quad (23)$$

$$DD^\# \mathbf{d} = \mathbf{d} \quad (24)$$

are satisfied, an analytic solution is given by Equation 25 and 26.

$$\mathbf{x} = D^\# \mathbf{d} + (I - D^\# D) \mathbf{w} \quad (25)$$

$$\mathbf{y} = B^\# \mathbf{c} - B^\# A D^\# \mathbf{d} - B^\# A (I - D^\# D) \mathbf{w} + (I - B^\# B) \mathbf{z} \quad (26)$$

Where  $\mathbf{w}$  is a vector of arbitrary integers and  $\mathbf{z}$  is an arbitrary vector of real numbers.

For a 2 dimensional test problem, consider pulsars with normal vectors  $[1, 0]^T$ ,  $[3/5, 4/5]^T$ ,  $[-4/5, 3/5]^T$ . For simplicity, the period and speed of light are normalized to 1 making the  $A$  matrix equal to the identity matrix and  $\mathbf{c}$  a vector of ones. The problem being considered is given by

$$\mathbf{x} + \begin{bmatrix} 1 & 0 \\ 3/5 & 4/5 \\ -4/5 & 3/5 \end{bmatrix} \mathbf{y} = \begin{bmatrix} 1 \\ 1 \\ 1 \end{bmatrix} \quad (27)$$

A reflexive generalized inverse of  $B$  which solves this problem is given by

$$B^\# = \begin{bmatrix} 1 & 0 & 0 \\ -3/4 & 5/4 & 0 \end{bmatrix} \quad (28)$$

The resulting  $\mathbf{d}$ ,  $D$ , and  $D^\#$  are given by

$$\mathbf{d} = \begin{bmatrix} 6 \\ 0 \\ 0 \end{bmatrix}, \quad D = \begin{bmatrix} -5 & 3 & -4 \\ 0 & 0 & 0 \\ 0 & 0 & 0 \end{bmatrix}, \quad D^\# = \begin{bmatrix} 1 & 0 & 0 \\ 2 & 0 & 0 \\ 0 & 0 & 0 \end{bmatrix} \quad (29)$$

Using these parameters, the solution to Equation 27 is given by

$$\mathbf{x} = \begin{bmatrix} 6w_1 - 3w_2 + 4w_3 + 6 \\ 10w_1 - 5w_2 + 8w_3 + 12 \\ w_3 \end{bmatrix} \quad (30)$$

$$\mathbf{y} = \begin{bmatrix} 6w_1 - 3w_2 + 4w_3 + 7 \\ 8w_1 - 4w_2 + 7w_3 + 11 \end{bmatrix} \quad (31)$$

By substituting integer values into  $w_1, w_2, w_3$  the candidate positions,  $\mathbf{y}$ , may be determined along with the pulsar index  $\mathbf{x}$ . In this case  $BB^\# = I$  makes the problem independent of  $\mathbf{z}$ , the vector of arbitrary numbers. One drawback of the analytic solution is that the candidate position vector is a  $2 \times 1$  vector ( $3 \times 1$  for 3 dimensional problems) and the  $w$  vector will be an  $N \times 1$  vector. Since this is the case, there is not a one-to-one correspondence between combinations of  $w_i$  and  $\mathbf{x}$ , thus a given candidate position may be found by multiple  $\mathbf{w}$  vectors.

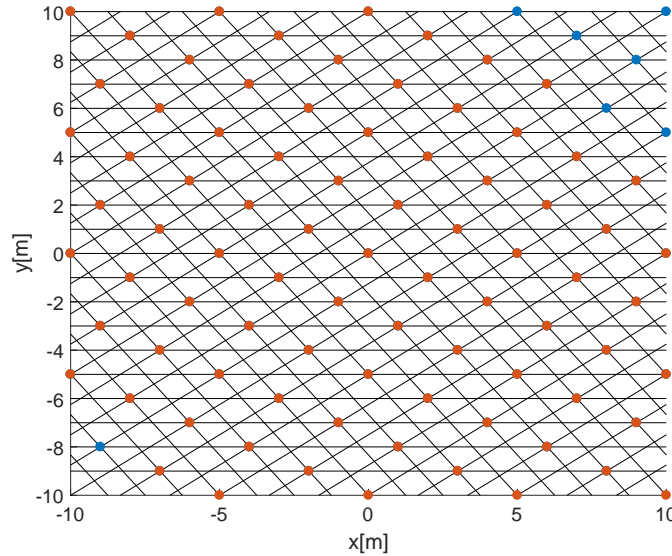


**Figure 8.** The intersection of three sets of lines are presented where the orange dots are analytically found intersections and the blue dots are additional intersections which were found numerically

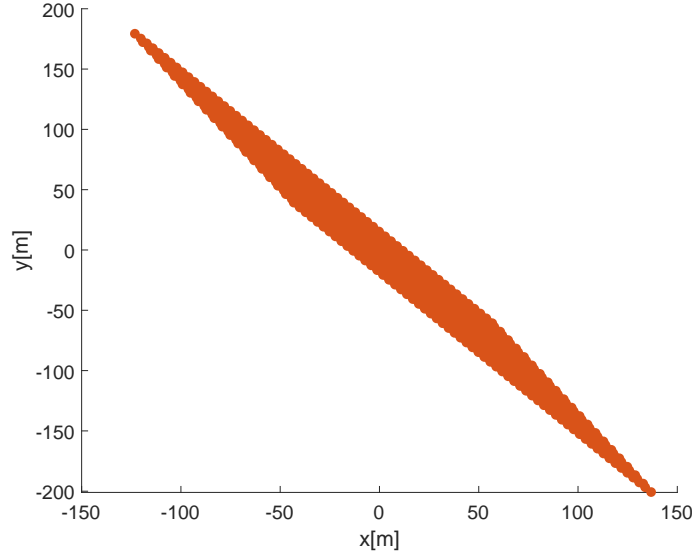


**Figure 9. Analytic solutions to the mixed integer problem outside of the domain**

Figure 8 shows the pulsar wavefronts and all analytic solutions are highlighted as orange dots. The blue dots represent additional solutions which may be found by using the numeric method, 84 solutions are found from the initial 140 candidate intersections resulting from 2 pulsars. Within the desired domain the analytic solution only finds 77 candidate solutions. Since there is no one-to-one correspondence between  $\mathbf{w}$  and  $\mathbf{x}$  there is no guarantee that all solutions in a given domain will be identified. In this case each  $w_i$  is varied independently from -10 to 10 resulting in  $21^3$  different values of  $\mathbf{w}$  and 9261 candidate solutions. Figure 9 shows the additional solutions that are found by the analytic method which lie outside of the domain in question. Of the 9261 analytic candidate solutions only 1281 are unique. The analytic solution also only finds exact solutions meaning there is no way to incorporate measurement error to find additional solutions.

## CONCLUSIONS

Two methods for determining candidate vehicle positions are presented for an XNAV system running in the absolute position update framework. This problem turns into finding the intersections of an infinite set of lines in two dimensions. The problem formulation is presented with a numeric algorithm which reduces the computational expense by a factor of  $N$ . Using this algorithm the candidate positions for three, four, and five pulsars are shown given a phase error between  $10^{-3}$  and  $10^{-5}$ . The cases where four pulsars are observed with a tolerance of  $10^{-5}$  and five pulsars are observed with a tolerance of  $10^{-3}$  both only have one solution within the domain. The solution with five pulsars and a phase accuracy of  $10^{-3}$  is the more appealing solution since the total observation time is smaller than that for one pulsar observation at  $10^{-5}$ . An analytic solution is also presented which finds an expression for exact solutions to the mixed-integer math problem. Unfortunately these solutions are parameterized by a non-unique vector of integers  $\mathbf{w}$  which does not guarantee all solutions within a particular domain will be found.

## REFERENCES

- [1] J. W. Mitchell, L. B. Winternitz, M. A. Hassouneh, S. R. Price, S. R. Semper, W. H. Yu, P. S. Ray, M. T. Wolff, M. Kerr, K. S. Wood, Z. Arzoumanian, K. C. Gendreau, and P. Demorest, "Sextant X-Ray Pulsar Navigation Demonstration: Initial On-Orbit Results," *AIAA Guidance and Control Conference*, Breckenridge, Colorado, 2018.
- [2] L. M. B. Winternitz, J. W. Mitchell, M. A. Hassouneh, S. R. Price, S. R. Semper, W. H. Yu, P. S. Ray, M. T. Wolff, M. Kerr, K. S. Wood, Z. Arzoumanian, K. C. Gendreau, L. Guillemot, P. Demorest, B. Stappers, and A. Lyne, "SEXTANT X-ray Pulsar Navigation Demonstration: Additional On-Orbit Results," *15th International Conference on Space Operations*, 2018, 10.2514/6.2018-2538.
- [3] S. Shemar, G. Fraser, L. Heil, D. Hindley, A. Martindale, P. Molyneux, J. Pye, R. Warwick, and A. Lamb, "Towards practical autonomous deep-space navigation using X-Ray pulsar timing," *Experimental Astronomy*, Vol. 42, No. 2, 2016, pp. 101–138, 10.1007/s10686-017-9552-3.
- [4] K. D. Anderson, D. J. Pines, and S. I. Sheikh, "Validation of Pulsar Phase Tracking for Spacecraft Navigation," *Journal of Guidance, Control, and Dynamics*, Vol. 38, No. 10, 2015, pp. 1885–1897, 10.2514/1.G000789.
- [5] D. W. Woodfork, *The Use of X-Ray Pulsar for Aiding GPS Satellite Orbit Determination*. PhD thesis, Air Force Institute of Technology, 2005, 10.1053/j.gastro.2015.08.053.
- [6] J. Liu, J. Ma, and J. Tian, "Pulsar/CNS integrated navigation based on federated UKF," *Journal of Systems Engineering and Electronics*, Vol. 21, No. 4, 2010, pp. 675–681, 10.3969/j.issn.1004-4132.2010.04.022.
- [7] X. Kai, W. Chunling, and L. Liangdong, "The use of X-ray pulsars for aiding navigation of satellites in constellations," *Acta Astronautica*, Vol. 64, No. 4, 2009, pp. 427–436, 10.1016/j.actaastro.2008.09.005.
- [8] S. I. Sheikh, *The use of Variable Celestial X-Ray Sources for Spacecraft Navigation*. PhD thesis, 2005.
- [9] S. I. Sheikh and D. J. Pines, "Recursive estimation of spacecraft position and velocity using X-ray pulsar time of arrival measurements," *Navigation, Journal of the Institute of Navigation*, Vol. 53, No. 3, 2006, pp. 149–166, 10.1002/j.2161-4296.2006.tb00380.x.
- [10] S. I. Sheikh, A. R. Golshan, and D. J. Pines, "Absolute and relative position determination using variable celestial X-ray sources," *30th Annual AAS Guidance and Control Conference*, 2007, pp. 855–874.
- [11] A. R. Golshan and S. I. Sheikh, "On pulse phase estimation and tracking of variable celestial X-ray sources," *Institute of Navigation 63rd Annual Meeting*, 2007, pp. 413–422, 10.1109/PLANS.2008.4570028.
- [12] V. Bowman and C.-A. Burdet, "On the General Solution to Systems of Mixed-Integer Linear Equations," *SIAM Journal on Applied Mathematics*, Vol. 26, No. 1, 1974, pp. 120–125.
- [13] M. F. Hurt and C. Waid, "A Generalized Inverse Which Gives all the Integral Solutions to a System of Linear Equations," *SIAM Journal on Applied Mathematics*, Vol. 19, No. 3, 1970, pp. 547–550, 10.1137/0119053.